Applied Geochemistry 24 (2009) 2195–2205

Contents lists available at ScienceDirect

Applied Geochemistry

journal homepage: www.elsevier.com/locate/apgeochem

Chemical weathering in Luzon, Philippines from clay mineralogy and major-element geochemistry of river sediments

Zhifei Liu [a,*], Yulong Zhao [a], Christophe Colin [b], Fernando P. Siringan [c], Qiong Wu [a]

[a] State Key Laboratory of Marine Geology, Tongji University, Shanghai 200092, China
[b] Laboratoire IDES, Bât. 504, UMR 8148 CNRS, Université de Paris XI, Orsay 91405, France
[c] Marine Science Institute, University of the Philippines, Diliman, Quezon City 1101, Philippines

ARTICLE INFO

Article history:
Received 3 April 2009
Accepted 23 September 2009
Available online 27 September 2009

Editorial handling by M. Hodson

ABSTRACT

Clay mineralogy and major-element geochemistry of 35 surface sediment samples collected in 21 major to moderate rivers of Luzon, Philippines are used to evaluate the present chemical weathering process. The clay mineral assemblage consists mainly of smectite (average 86%) with minor kaolinite (9%) and chlorite (5%) and very scarce illite (1%), and does not show strong island-wide differences. The major element results of both bulk and clay-fraction sediments indicate that the formation of clay minerals is accompanied by leaching of Ca and Na first and of Fe and Mn thereafter during the chemical weathering process. A low-moderate chemical weathering degree of bulk sediments and a moderate-intensive degree of clay-fraction sediments are obtained in Luzon rivers based on proxies of chemical index of alteration (CIA) and smectite crystallinity. It is suggested that the majority of andesitic–basaltic volcanic and sedimentary rocks along with the tectonically active geological setting and sub-tropical East Asian monsoon climate are responsible for the predominance of smectite in the clay mineral assemblage.

1. Introduction

Weathering products of silicate rocks are particularly useful for evaluating the continental chemical weathering that acts as a net sink for atmospheric CO_2 (Walker et al., 1981; Louvat and Allègre, 1998). The most abundant weathering products are generated in the region of SE Asia, where the fluvial systems have the highest denudation rates in the world (McLennan, 1993; Summerfield and Hulton, 1994) and supply as much as 70% of the global suspended sediment to the world ocean (Milliman and Meade, 1983; Milliman and Syvitski, 1992). Previous studies of chemical weathering based on river sediments have been carried out in numerous rivers in the region, like the Yangtze and Yellow rivers in North China (Yang et al., 2004), the Pearl, Red and Mekong rivers in South China and Indochina (Liu et al., 2007a), the Ganges–Brahmaputra River system in South Asia (Galy and France-Lanord, 1999; Singh et al., 2005), and mountainous rivers in SW Taiwan (Selvaraj and Chen, 2006; Liu et al., 2008). However, few studies have been conducted on weathering products in the Philippine archipelago, where the weathering of volcanic rocks could be particularly efficient, as shown in studies of large basaltic provinces on the Deccan Traps (Dessert et al., 2001) and in NE Iceland (Eiriksdottir et al., 2008). As the largest island in the Philippines, Luzon is an intermediate-basaltic volcanic and tectonically active island characterized by high relief, heavy rainfall, and warm temperature. Therefore, Luzon is an excellent area to examine the present chemical weathering process of volcanic rocks.

In this study, clay mineralogy and major-element geochemistry have been investigated for the first time on modern argillaceous sediments from all major to moderate rivers in Luzon. To obtain trends of chemical weathering, major elements were analyzed not only in bulk but also in clay-fraction particles. Major element results were then combined with clay mineralogical proxies (clay mineral contents and smectite crystallinity) to quantify chemical weathering states for the river sediments in Luzon.

2. Geological and hydrographic settings

Luzon is situated in a rapidly deforming island arc, where convergence between the Eurasian Plate (Sundaland block) and the Philippine Sea Plate is accommodated across two major subduction zones, the east-dipping Manila Trench in the eastern South China Sea and the west-dipping East Luzon Trough in the western Pacific Ocean (Fig. 1). The island is characterized by active intra-arc strike-slip faults, active volcanism, and high seismic activity. Cretaceous to Quaternary sedimentary and extrusive rocks and Cenozoic intermediate intrusive rocks abound throughout the island (Commission for the Geological Map of the World, 1975) (Fig. 2A). Sedimentary rocks usually contain andesitic–basaltic pyroclastics and lavas. Plio-Quaternary volcanic deposits, mostly andesites and basalts with associated dacites and rhyodacites, mainly occur

* Corresponding author. Fax: +86 21 6598 8808.
E-mail address: lzhifei@tongji.edu.cn (Z. Liu).

0883-2927/$ - see front matter © 2009 Elsevier Ltd. All rights reserved.
doi:10.1016/j.apgeochem.2009.09.025

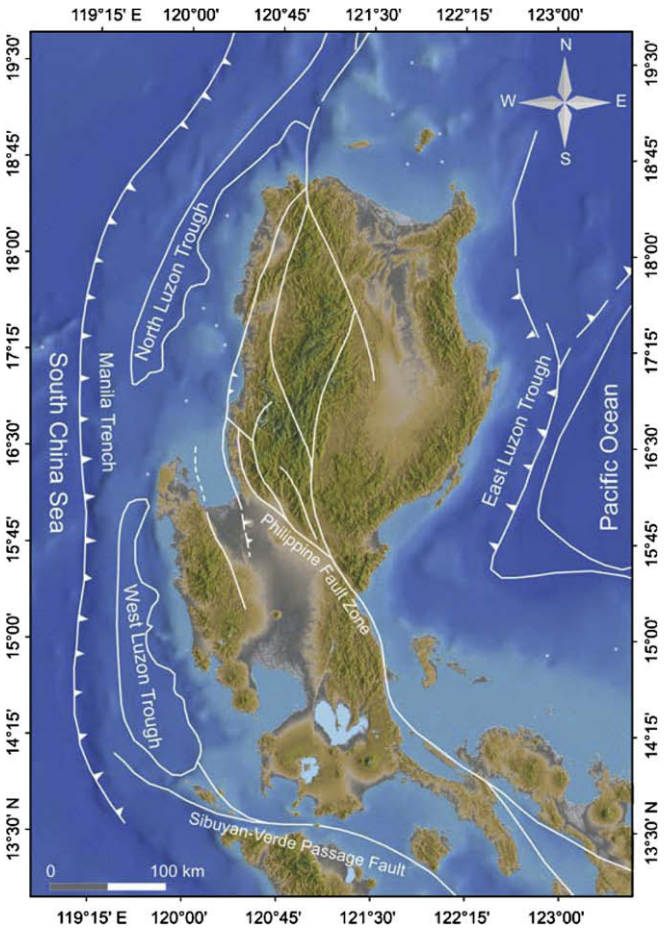

Fig. 1. Tectonic setting of Luzon (modified after Rimando and Knuepfer, 2006).

in southern Luzon. In contrast, Cretaceous-Paleogene undifferentiated strata, commonly mapped as volcanics, are distributed in most mountainous regions of Luzon. Cenozoic intermediate-acid intrusive rocks, mainly as diorite, granodiorite, and quartz diorite, are associated with the undifferentiated Cretaceous-Paleogene volcanic rocks (Fig. 2A). Adakites and adakitic rocks have also been identified among the intrusive rocks (Bellon and Yumul, 2001). In addition, two blocks of Mesozoic ultrabasics, mainly peridotite, dunite and layered gabbro, are located at the eastern and southwestern margins of Luzon. A patch of Paleozoic metamorphic rocks also developed at the eastern margin (Fig. 2A).

The region of Luzon is dominated by the sub-tropical East Asian monsoon climate, with an annual heavy rainfall of 1900–2100 mm (Fig. 3). Rain everywhere is seasonal, with nearly 85–90% of the annual rainfall arriving during the summer monsoon season between May and October. Temperature varies between 23 and 34 °C in both winter and summer, with a maximum of 34 °C in middle April (http://www.worldweather.org). Fluvial drainage systems are well developed in the region (Fig. 2A). In terms of drainage area and mean daily discharge, the largest river is the Cagayan River that mostly drains through surrounding mountainous areas in northern Luzon, and flows northward to the Luzon Strait (Table 1, Fig. 2A). Its mean discharge (1.5×10^3 cm^3/s) is much smaller than the world's largest rivers, like the Pearl River with an average discharge of approximately 10×10^9 cm^3/s (Harrison et al., 2008). Cretaceous to Quaternary sedimentary and volcanic rocks and Cenozoic intermediate intrusive rocks occur in the drainage basin (Fig. 2A). In term of drainage area, the Pampanga River is the second largest river that drains southward in southern Luzon into Manila Bay. The Holocene to Miocene sedimentary rocks and Plio-Quaternary volcanic deposits are the major lithologies of the basin. The Vigan River in the NW and the Agno River in the SW drain through western Luzon and then flow into the South China Sea. The Mesozoic ultrabasic intrusive body developed in the Agno River drainage basin. In addition, there are more than 15 moderate rivers developed in western Luzon and draining into the South China Sea. Because of the incompleteness of hydrological data from the Luzon rivers, values of the suspended sediment yield of all rivers are not available, except the Pampanga River and the Ango River with 3.50×10^6 and 4.70×10^6 t/a, respectively (Table 1).

3. Sampling and analytical methods

Muddy channel deposits were sampled in July 2007. Thirty five samples were collected at 35 different locations from all 21 major to moderate rivers (Fig. 2B, Table 2). Sampling sites were chosen to avoid contamination from riverbank sediments. Surface argillaceous sediments were taken either on a river beach near water or on a river bottom below shallow water. For practical purposes and considering the similar geological settings, all of the 21 major to moderate rivers are grouped into four river systems (Fig. 2B, Table 2): (1) Pampanga River system, including the Pampanga River and one moderate river draining into Manila Bay; (2) Agno River system, including the Agno River and another seven moderate rivers draining into the South China Sea in southwestern Luzon; (3) Vigan River system, including the Vigan River and another eight moderate rivers draining into the South China Sea in northwestern Luzon; (4) Cagayan River system, including the Cagayan River and one moderate river draining to the Luzon Strait. All samples were analyzed for clay minerals (<2 μm) and major elements in both bulk (<63 μm) and clay-fraction (<2 μm) particles.

Clay minerals were identified by X-ray diffraction (XRD) using a PANalytical diffractometer at the Laboratoire IDES, Université de Paris XI on oriented mounts of non-calcareous clay-sized (<2 μm) particles (Holtzapffel, 1985). The oriented mounts were obtained following the methods described in detail by Liu et al. (2004). Three XRD runs were performed, following air-drying, ethyleneglycol solvation for 24 h, and heating at 490 °C for 2 h. Identification of clay minerals was made mainly according to the position of the (0 0 1) series of basal reflections on the 3 XRD diagrams. Semi-quantitative estimates of peak areas of the basal reflections for the main clay mineral groups of smectite (including mixed-layers) (15–17 Å), illite (10 Å), and kaolinite/chlorite (7 Å) were carried out on the glycolated curve (Holtzapffel, 1985) using the MacDiff software (Petschick, 2000). Relative proportions of kaolinite and chlorite were determined based on the ratio from the 3.57/3.54 Å peak areas. Following the laboratory routine (Liu et al., 2004, 2007a,b), the weighting factors introduced by Biscaye (1965) are not used when generating relative weight percentages of each clay mineral. Replicate analyses of a few selected samples gave a precision of ±2% (2σ). Based upon the XRD method, the semi-quantitative evaluation of each clay mineral has an accuracy of ~5%. Additionally, smectite crystallinity was obtained from half height width of the 17 Å peak on the glycolated curve. Higher values represent the lower crystallinity, characteristic of strong hydrolysis in continental sources and humid and warm climate conditions (Chamley, 1989). Smectite crystallinity can be also used to indentify the occurrence of mixed-layers that may modify significantly the apparent crystallinity.

Major elements were measured by inductively coupled plasma-optical emission (ICP-OES) using an IRIS Advantage at the State Key Laboratory of Marine Geology, Tongji University on carbonate- and organic-free bulk (<63 μm) and clay-fraction (<2 μm) particles. Organic matter and calcite were removed using 10% H_2O_2 and 1% HCl,

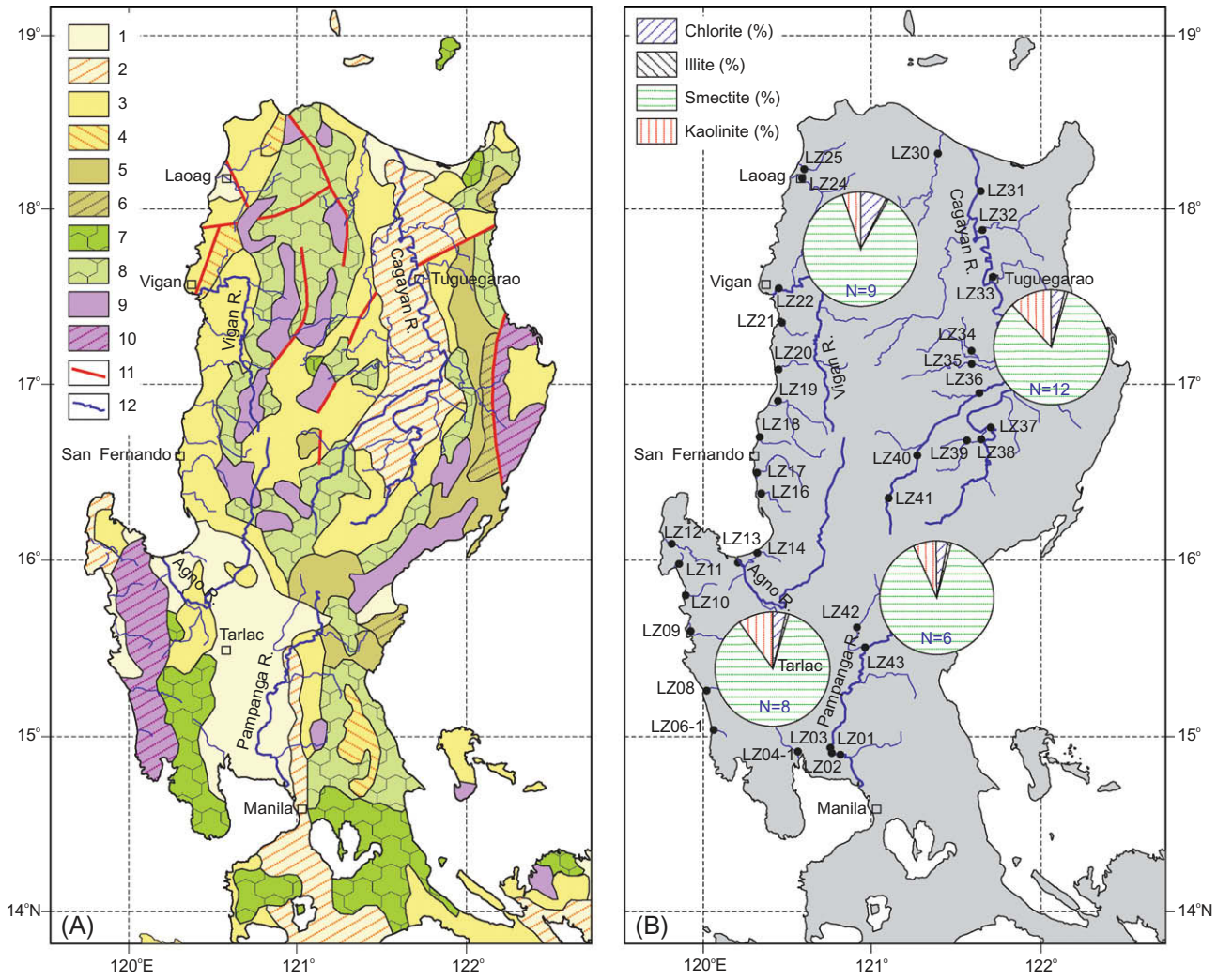

Fig. 2. (A) Geological map of Luzon (modified after Commission for the Geological Map of the World, 1975). 1. Holocene sediments; 2. Plio-Pleistocene sediments; 3. Miocene sedimentary rocks; 4. Paleogene sedimentary rocks; 5. Cretaceous-Tertiary sedimentary rocks; 6. Paleozoic metamorphic rocks; 7. Plio-Quaternary extrusive rocks; 8. Cretaceous-Paleogene extrusive rocks; 9. Cenozoic intermediate intrusive rocks; 10. Mesozoic ultrabasic intrusive rocks; 11. Faults; 12. Rivers. (B) Locations of river surface sediments and distribution of average clay mineral assemblages of four river systems. See Table 2 for detailed GPS positions and clay mineral proportions. *N* = number of surface samples.

respectively, in order to purify granule silicate particles. Particles <63 μm were wet sieved to remove potential local coarse grains that may significantly change the general geochemical composition. The experiments indicate that there are almost no particles >63 μm in the original argillaceous samples. Clay-fraction (<2 μm) particles were isolated from deflocculated suspensions using Stoke's Law in a settling beaker. Sieved bulk particles and isolated clay fractions were then centrifuged and the resulting paste was oven dried at 60 °C. About 30–40 mg pre-prepared sediments were heated at 600 °C to obtain the loss of ignition (LOI), and then were dissolved using a mixture solution of HNO_3 + HF on a hot plate. The eluted sample was diluted with 2% HNO_3 for the major-element measurement. This preparation procedure does not allow measuring Si directly using ICP-OES, and the concentrations of SiO_2 were obtained by difference to 100% subtracting all other major-element concentrations and LOI. Replicate analyses ($N = 20$) of GSR-5, GSR-6, GSD-9 and GSD-12 reference samples during the study gave an accuracy of 10% for Si and of 4% for all other major elements. Replicate analyses of selected samples gave a precision of ±3% (2σ) for bulk particles and ±1% (2σ) for clay fractions.

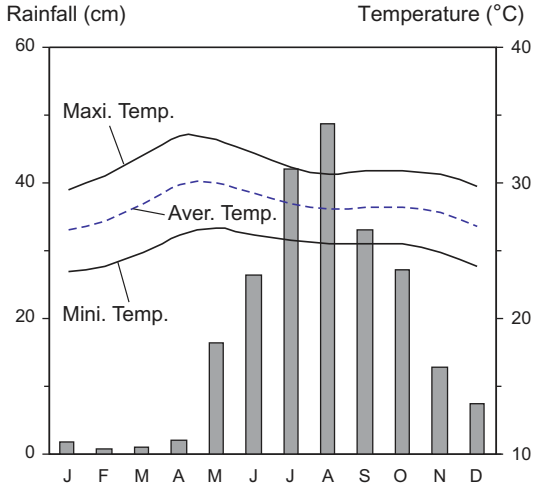

Fig. 3. Rainfall and temperature distribution at Manila in southern Luzon. Monthly average data between 1971 and 2000 were obtained online through the World Weather Information Service (http://www.worldweather.org).

4. Results

4.1. Clay minerals

The clay mineral assemblages in all major to moderate rivers of Luzon are similar, dominantly consisting of smectite (60–97%) with an average content of 86%; kaolinite (0–39%) and chlorite (0–35%) present in much lesser abundance with average contents of 9% and 5%, respectively; illite (0–3%) is very scarce with an average content of 1%. Rarely, halloysite, saponite, anorthite, talc, clinochrysotile, and clinoptilolite in clay fractions were also detected in some samples (Table 2; Fig. 4). Saponite is a trioctahedral (Mg-type) smectite and it is not included in "smectite" throughout the text, which is mainly the dioctahedral (Al–Fe type) smectite according to their elemental geochemistry. A small amount of quartz exists in most of the clay fractions samples. The predominance of smectite in most of the samples is impressive when compared to other minerals on the XRD diagrams (Fig. 4). The distribution of average clay mineral assemblages has been calculated for the four river systems (Fig. 2B, Table 3). The Pampanga River system in southern Luzon contains the relatively highest content of smectite (average 89%), while the Cagayan River system in northern Luzon has the lowest content (83%), but the highest content of kaolinite (12%). The Agno River and Vigan River systems in western Luzon contain rare talc, clinochrysotile and clinoptilolite minerals (Table 2). Low concentrations of halloysite are common in all river systems (Table 2). Smectite crystallinity varies between 0.40 and 1.88°$\Delta 2\theta$, with relatively low values in the Vigan River system and high values in the Cagayan River system (Tables 2 and 3). The smooth shape of the 17 Å peak on the glycolated curve (e.g. Fig. 4) indicates that smectite-related mixed-layers are very rare in most of the river samples. Therefore, the smectite crystallinity (half height width) is not affected by the occurrence of mixed-layers, and can be efficiently implied to represent the chemical weathering intensity.

4.2. Major elements

The bulk and clay-fraction carbonate-free surface sediments from all major to moderate rivers of Luzon are characterized by high contents of SiO_2, Al_2O_3, and Fe_2O_3, and by low concentrations of CaO, K_2O, MgO, MnO, Na_2O, P_2O_5 and TiO_2 (Table 4). Clay-fraction sediments usually contain higher Al_2O_3, Fe_2O_3 and TiO_2, and lower SiO_2, CaO, K_2O and Na_2O than bulk sediments. They have been plotted on variation diagrams using Al_2O_3 along the x axis (Fig. 5). Data for upper continental crust (UCC) from Taylor and McLennan (1985) were also plotted as a reference. Generally, clay-fraction sediments have stronger correlations than bulk sediments for most major elements (Fig. 5). Moderate to strong negative correlations between Al_2O_3 and SiO_2 and CaO in both bulk and clay fractions indicate mineralogical control on SiO_2 and CaO contents, because quartz- and anorthite-rich mineral associations often produce higher SiO_2 and CaO concentrations, respectively. Moderate negative correlations are also found in diagrams of Al_2O_3 versus K_2O and Na_2O in clay-fraction sediments, suggesting the leaching of the mobile elements K and Na during the formation of clay minerals. However, diagrams of Al_2O_3 versus Fe_2O_3 and TiO_2 display moderate positive correlations, indicating enrichment of the immobile elements Fe and Ti during chemical weathering of river sediments. There is a great dispersion in diagrams of Al_2O_3 versus MgO, MnO and P_2O_5. Among the different river systems (Fig. 5), the Agno River system gives a more scattered distribution for most major elements in both bulk and clay-fraction sediments. No significant difference in major element compositions is observed in the other 3 river systems.

5. Discussion

5.1. Formation of smectite

The dominant occurrence of smectite throughout rivers in Luzon suggests lithology- and climate-controlled clay mineral assemblages. Under hot and humid climate conditions, weathering tends to progress on volcanic rocks faster than on most other rocks (Bluth and Kump, 1994; Dessert et al., 2001). The abundance of amorphous materials facilitates hydrolysis and the frequency of porous rocks favors leaching and drainage (Chamley, 1989). The rapidity of volcanic rock weathering often induces a high abundance of smectite that forms easily on andesitic–basaltic materials as Fe–Mg species and on rhyolitic materials rather than as Al species. Fairly-well to very-well-crystallized smectite forms abundantly on volcanic rocks under a temperate-warm to cool climate (Chamley, 1989). Four steps of clay mineral formation can be recognized in volcanic environments depending on climate, drainage, local petrography, and duration of weathering (Chamley, 1989): (1) formation of amorphous to sub-amorphous clays, like allophane and imorgolite; (2) widespread development of Fe- to Al-smectite (nontronite, montmorillonite, etc.); (3) increase in halloysite, a hydrated form of kaolinite; (4) increased kaolinization, often associated with the formation of gibbsite, characteristic of the last step of andosol development.

The majority of andesitic–basaltic volcanic and sedimentary rocks in Luzon (Fig. 2A) can be strongly eroded under the tectonically active setting (active strike-slip faults, active volcanism, and high seismic activity). The sub-tropical East Asian monsoon climate with heavy rainfall during May–October and consistency of hot-warm temperature throughout the year (Fig. 3) allow for the intense chemical weathering. Both lithology and climate conditions can be used to interpret the predominance of smectite in all major to moderate rivers in Luzon (Fig. 2B). The very well-crystallized smectite with relatively low values of smectite crystallinity (Table 2) can be generated as soon as the chemical weathering starts. Strong erosion along with heavy monsoon rainfall, then, may frequently remove the weathered smectite soil from rock surfaces, preventing the widespread formation of halloysite and kaolinite, which would indicate more intense in situ weathering. But at a few locations, kaolinite contents can reach 14–18% (Table 2), which is attributed to high rainfall with a short but significant dry season most likely in April–May with the highest temperature during the beginning of the heavy rainfall (Fig. 3). The common occurrence of low concentrations of halloysite may be attributed

Table 1
Drainage area, mean daily discharge, and annual sediment yield of four largest drainage basins in Luzon.

River drainage basin	Drainage area (km^2)	Mean discharge (cm^3/s)	Annual sediment yield (10^6 tons/year)	Period covered
Pampanga River	8625	240.82	3.50	1971–1979
Agno River	6340	211.17	4.70	[a]
Vigan River	5208	347.51	[a]	1959–1976
Cagayan River	30,416	1487.64	[a]	1984–1990

[a] Not available.

Table 2
Geographic locations and clay mineral assemblages of surface sediments in Luzon rivers.

No.	Sample	River	Location	Latitude (N)	Longitude (E)	Smectite (%)	Illite (%)	Kaolinite (%)	Chlorite (%)	Smectite crystallinity (°Δ2θ)	Halloysite	Saponite	Anorthite	Talc	Clinochrysotile	Clinoptilolite
Pampanga River system																
1	LZ01	Angat R. (Trib. Pampanga R.)	Tibag	14°54′8.0″	120°49′8.7″	86	1	5	8	0.91	X	X				
2	LZ02	Pampanga R.	Calumpn	14°55′5.8″	120°46′6.4″	91	1	4	4	1.05	X	X				
3	LZ03	Pampanga R.	Apalit	14°56′19.6″	120°45′37.9″	90	1	5	5	0.88	X	X				
4	LZ04-1	Lubao R.	Lubao	14°54′57.4″	120°34′6.7″	91	2	4	4	0.72			X			
5	LZ42	Talavera (Trib. Pampanga R.)	Talavera	15°36′37.1″	120°55′11.6″	86	0	14	0	1.26	X					
6	LZ43	Pampanga R.	Cabanatuan	15°30′52.8″	120°57′21.9″	91	1	8	0	0.99	X	X	X			
Agno River system																
7	LZ06-1	Santo Tomas R.	San Narciso	15°2′1.9″	120°4′32.8″	92	3	5	0	0.40			X			
8	LZ08	Bucao R.	Botolan	15°15′42.1″	120°2′13.3″	80	1	19	0	0.85	X		X	X		
9	LZ09	Lauis R.	Candelaria	15°35′46.4″	119°56′32.7″	79	0	9	12	0.82				X	X	
10	LZ10	Nayom R.	Santa Cruz	15°48′31.9″	119°54′53.8″	78	0	22	0	0.96	X			X		
11	LZ11	Dasol R.	Dasol	15°59′30.9″	119°52′23.4″	96	0	4	0	1.88	X	X				
12	LZ12	Balincaguin R.	Burgos	16°4′31.0″	119°53′37.3″	86	0	8	7	0.67	X	X		X		
13	LZ13	Agno R.	Lingayen	15°58′47.2″	120°13′33.4″	87	2	6	6	1.01	X	X	X			
14	LZ14	San Pablo R.	Dagupan City	16°1′52.6″	120°20′33.9″	90	1	5	4	1.05	X	X	X			
Vigan River system																
15	LZ16	Aringay R.	Aringay	16°23′26.0″	120°21′30.0″	97	0	3	0	1.28	X	X				X
16	LZ17	Bauang R.	Bauang	16°31′0.8″	120°19′53.2″	94	0	5	0	0.95	X	X				X
17	LZ18	Baroro R.	Bacnotan	16°42′42.7″	120°20′40.0″	93	0	6	0	1.09	X	X	X			X
18	LZ19	Amburayang R.	Sudipen	14°54′50.3″	120°27′44.0″	91	1	0	7	0.59	X		X			X
19	LZ20	Santa Cruz R.	Santa Cruz	17°5′39.7″	120°27′33.5″	93	1	3	3	0.72	X	X	X			X
20	LZ21	Santa Maria R.	Santa Maria	17°23′11.0″	120°29′2.2″	95	1	4	0	0.95	X		X			X
21	LZ22	Vigan R.	Vigan	17°33′32.1″	120°28′1.0″	66	2	17	15	0.74	X	X	X			
22	LZ24	Laoag R.	Laoag City	18°11′33.6″	120°35′32.0″	65	0	0	35	1.02						X
23	LZ25	Vintar R.	Bacarra	18°14′51.2”	120°37′22.6″	86	1	7	6	0.78	X	X				X
Cagayan River system																
24	LZ30	Abulug R.	Lucban	18°20′17.2″	121°25′33.1″	71	3	0	26	0.75						
25	LZ31	Cagayan R.	Gattaran	18°7′22.0″	121°40′24.1″	89	1	10	0	1.09	X	X	X			
26	LZ32	Trib. Cagayan R.	Alcala	17°53′38.2″	121°41′16.2″	92	1	8	0	0.94	X					X
27	LZ33-1	Cagayan R.	Tuguegarao	17°36′50.8″	121°41′27.2″	80	1	12	7	1.12	X	X	X			X
28	LZ34	Malig R. (Trib. Cagayan R.)	Mallig	17°10′29.4″	121°36′39.7″	94	0	6	0	0.98	X					
29	LZ35	Siffu (Trib. Cagayan R.)	Roxas	17°7′48.3″	121°36′51.6″	93	1	6	0	0.91	X		X			X
30	LZ36	Magat R. (Trib. Cagayan R.)	Cabatuan	16°58′19.3″	121°39′24.6″	95	0	5	0	1.40	X	X				
31	LZ37	Cagayan R.	Angadanan	16°44′49.4″	121°44′42.2″	83	1	16	0	1.26	X		X			
32	LZ38	Ganano R. (Trib. Cagayan R.)	Ganano	16°46′11.5″	121°41′53.8″	84	0	16	0	1.28	X		X			
33	LZ39	Santiago R. (Trib. Cagayan R.)	Santiago	16°41′44.9″	121°33′21.5″	81	1	18	0	1.33	X		X			
34	LZ40	Magat R. (Trib. Cagayan R.)	Bayombong	16°35′12.8″	121°16′2.5″	76	3	9	13	1.00			X			
35	LZ41	Magat R. (Trib. Cagayan R.)	Bambang	16°21′48.9″	121°5′39.1″	60	1	39	0	1.20	X					

X = Low concentration, <0.5%.

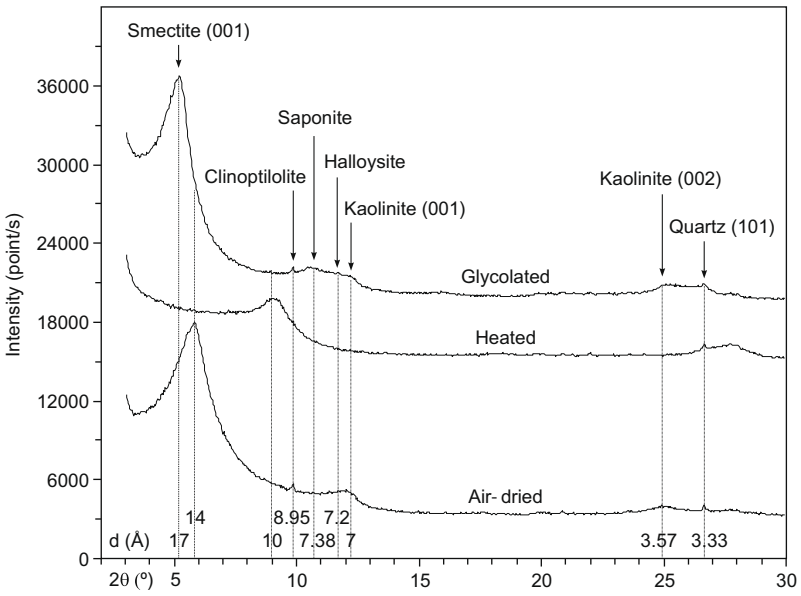

Fig. 4. Multiple X-ray diffractograms of a typical sample (LZ16) from the Aringay River in western Luzon. The sample contains predominantly smectite with little kaolinite, halloysite, clinoptilolite, saponite, and quartz. See Table 2 for clay mineral assemblage of this sample.

Table 3
Average clay mineral assemblage of surface sediments in four Luzon river systems.

River system	Sample number	Smectite (%)	Illite (%)	Kaolinite (%)	Chlorite (%)	Smectite crystallinity (°Δ2θ)
Pampanga River system	6	89	1	7	3	0.97
Agno River system	8	86	1	10	3	0.95
Vigan River system	9	87	1	5	7	0.90
Cagayan River system	12	83	1	12	4	1.10

to conditions of high Si concentration within microenvironments containing feldspar and pumice pseudomorphs (Kleber et al., 2007). In brief, the formation of clay minerals in Luzon falls mainly in widespread development of smectite (Step 2) associated with less significant development of halloysite and kaolinite (Step 3) following the description of Chamley (1989). Conditions of halloysite formation require further research.

Besides the predominant clay mineral smectite associated with much less abundant kaolinite and chlorite and scarce illite and halloysite, low concentrations of talc, clinochrysotile and clinoptilolite are also present (Table 2). Talc and clinochrysotile as characteristic weathering products of peridotite, dunite and gabbro, develop only in the Agno River system. Their occurrence can be attributed to chemical weathering of the ultrabasic intrusive rocks situated in the source area at the southwestern margin of Luzon (Fig. 2A). Clinoptilolite commonly occurs as an authigenic devitrification product of volcanic glass shards in tuff and as vesicle fillings in basalts and andesites. This mineral is widely scattered in northern Luzon, where volcanic rocks mainly outcrop.

The clay mineral assemblage of Luzon rivers is very different from those of other rivers in Southeast Asia (Fig. 6). Luzon rivers show a clear predominance of smectite (86%) and minor portions of kaolinite (9%) and chlorite (5%). Rivers in southwestern Taiwan carry mainly illite and chlorite up to ~100% (Liu et al., 2008). The Pearl, Red, and Mekong rivers in South China and Indochina Peninsula have an illite–chlorite–kaolinite assemblage with higher contents of kaolinite in the Pearl River, but much less abundance of smectite for all three rivers (Liu et al., 2007a). While in Borneo rivers, illite and chlorite (~88%) make up the major contribution to clay minerals with associated kaolintie (12%) and little smectite (Liu et al., 2007b). Therefore, with the predominance of smectite, Luzon is often viewed as an end-member for source analysis of detrital fine-grained sediments in the South China Sea (Boulay et al., 2005; Wan et al., 2007; Liu et al., 2008).

5.2. Chemical mobility and weathering trends

The chemical composition of weathering products in a river basin is expected to demonstrate well-established concepts on mobility of various elements during weathering (Nesbitt et al., 1980; Singh et al., 2005), and therefore to assess the state of chemical and physical weathering (Vital and Stattegger, 2000; Singh et al., 2005; Liu et al., 2007a). Here elemental ratios calculated with respect to Al are used to identify and evaluate the major element mobility. The ratio of the content of element X and Al_2O_3 in river samples divided by the ratio of the same element content of UCC gives the following elemental ratio (Singh et al., 2005):

$$\text{Elemental ratio } (X) = \frac{X/Al_2O_3(\text{rivers})}{X/Al_2O_3(\text{UCC})}.$$

The elemental ratio refers to the relative enrichment or depletion of the element, i.e., >1 indicates enrichment, <1 indicates depletion, and =1 indicates no change in the relative abundance of the element.

The elemental ratios calculated from average major-element concentrations normalized to UCC are displayed in Fig. 7. All major elements from both bulk and clay-fraction sediments show similar chemical mobility with little differences. In general, clay-fraction

Table 4
Major element composition (%) of bulk (<63 μm) and clay-fraction (<2 μm) sediments in Luzon rivers.

No.	Sample	Al_2O_3	CaO	Fe_2O_3	K_2O	MgO	MnO	Na_2O	P_2O_5	TiO_2	SiO_2	LOI	CIA
Bulk (<63 μm) sediments													
Pampanga River system													
1	LZ01	16.89	2.50	9.47	0.84	3.26	0.11	2.12	0.24	1.00	57.39	6.18	65.36
2	LZ02	16.14	2.50	10.15	0.80	2.81	0.12	2.12	0.49	0.85	56.92	7.10	64.45
3	LZ03	17.19	3.06	8.65	0.94	3.05	0.12	2.16	0.15	0.77	56.78	7.13	62.90
4	LZ04-1	16.69	3.62	5.38	1.18	2.23	0.09	3.38	0.16	0.61	63.88	2.77	55.40
5	LZ42	16.48	3.48	8.44	0.48	2.50	0.17	2.10	0.11	0.84	58.59	6.81	61.50
6	LZ43	15.90	3.27	8.61	0.49	2.29	0.22	2.09	0.10	0.87	60.43	5.73	61.55
Agno River system													
7	LZ06-1	13.95	2.67	3.03	2.34	1.74	0.08	3.68	0.10	0.33	69.66	2.43	50.90
8	LZ08	15.20	2.05	5.60	1.69	2.43	0.08	2.69	0.13	0.31	64.30	5.50	60.30
9	LZ09	8.97	3.84	10.42	0.00	17.55	0.12	0.52	0.05	0.28	51.04	7.19	53.30
10	LZ10	15.97	5.15	10.00	0.07	7.87	0.11	0.75	0.04	0.33	52.86	6.84	59.90
11	LZ11	13.49	6.27	8.35	0.49	2.74	0.07	1.24	0.12	0.60	55.10	11.52	49.08
12	LZ12	14.63	5.01	10.65	0.12	6.87	0.13	1.15	0.05	0.49	55.47	5.42	56.74
13	LZ13	17.59	2.43	8.96	0.85	3.52	0.17	2.16	0.11	0.75	56.25	7.20	66.41
14	LZ14	17.59	2.67	8.14	0.84	2.94	0.14	2.21	0.17	0.79	58.30	6.20	65.17
Vigan River system													
15	LZ16	18.58	1.80	8.05	0.88	2.48	0.09	1.22	0.17	0.71	57.28	8.74	74.89
16	LZ17	18.28	2.62	7.91	0.96	2.76	0.10	1.52	0.20	0.72	57.16	7.78	68.78
17	LZ18	18.22	2.05	8.10	1.07	2.93	0.18	1.42	0.25	0.67	55.92	9.19	71.60
18	LZ19	17.62	2.61	7.39	0.82	3.23	0.09	1.75	0.18	0.70	58.06	7.56	67.40
19	LZ20	15.73	6.08	7.68	1.07	3.58	0.13	1.69	0.19	0.66	54.96	8.22	51.14
20	LZ21	16.24	4.47	7.58	1.22	2.92	0.11	1.42	0.17	0.66	56.16	9.04	57.92
21	LZ22	19.33	2.66	8.73	0.64	2.66	0.14	1.51	0.17	0.83	53.77	9.56	70.69
22	LZ24	17.33	3.16	9.80	0.45	3.12	0.16	1.92	0.17	0.84	54.98	8.09	64.83
23	LZ25	16.68	3.99	9.38	0.57	2.78	0.14	1.13	0.16	0.80	51.39	12.98	63.14
Cagayan River system													
24	LZ30	17.35	2.94	8.21	0.80	3.17	0.15	2.36	0.18	0.85	56.75	7.25	63.23
25	LZ31	17.90	2.34	8.47	1.12	2.44	0.15	1.44	0.17	0.83	56.48	8.65	69.50
26	LZ32	16.44	5.63	9.68	0.92	2.95	0.16	1.13	0.15	0.87	51.47	10.61	55.63
27	LZ33-1	18.57	2.38	8.44	0.99	2.47	0.12	1.69	0.16	0.80	57.16	7.23	69.43
28	LZ34	16.71	3.24	8.32	1.77	2.78	0.13	1.85	0.19	0.76	56.66	7.60	60.62
29	LZ35	17.00	3.83	8.16	2.01	2.86	0.14	1.52	0.25	0.72	56.26	7.24	59.31
30	LZ36	16.65	2.12	8.00	1.88	2.12	0.16	0.98	0.18	0.75	58.50	8.66	68.93
31	LZ37	17.79	1.37	8.55	1.49	1.50	0.20	0.85	0.22	0.84	56.43	10.74	76.30
32	LZ38	16.76	1.86	8.17	1.79	1.53	0.55	1.02	0.25	0.79	58.00	9.28	70.53
33	LZ39	16.87	1.67	9.25	3.22	1.12	0.51	1.09	0.29	0.81	56.60	8.56	66.94
34	LZ40	17.31	4.05	8.49	1.31	3.20	0.17	1.92	0.19	0.83	53.93	8.59	59.14
35	LZ41	18.14	2.44	8.56	0.69	2.19	0.16	1.84	0.16	0.75	57.16	7.91	68.84
Clay-fraction (<2 μm) sediments													
Pampanga River system													
1	LZ01	20.38	0.92	12.03	0.75	3.24	0.11	0.85	0.48	1.05	49.42	10.77	83.96
2	LZ02	19.03	0.83	13.50	0.68	2.86	0.13	0.72	0.85	0.99	49.95	10.47	84.74
3	LZ03	19.13	1.74	11.37	0.76	3.55	0.14	0.77	0.23	0.94	50.35	11.01	78.44
4	LZ04-1	18.61	1.03	7.96	1.12	2.33	0.09	1.44	0.51	0.69	57.34	8.89	77.31
5	LZ42	19.86	1.71	10.18	0.43	2.50	0.17	0.60	0.14	0.89	52.44	11.09	81.29
6	LZ43	19.75	1.50	10.78	0.40	2.38	0.25	0.50	0.12	0.90	51.84	11.59	83.23
Agno River system													
7	LZ06-1	14.23	1.95	4.21	2.23	2.37	0.09	2.98	0.27	0.35	67.14	4.18	56.72
8	LZ08	18.50	1.20	9.70	0.77	2.83	0.09	1.07	0.30	0.33	55.55	9.67	79.50
9	LZ09	11.54	0.83	13.67	0.03	11.74	0.09	0.18	0.11	0.22	48.80	12.77	86.20
10	LZ10	21.72	0.98	11.16	0.09	3.34	0.07	0.34	0.07	0.30	47.80	14.14	89.87
11	LZ11	17.87	3.42	10.33	0.43	2.81	0.07	0.36	0.17	0.62	49.80	14.13	71.07
12	LZ12	20.13	1.15	11.48	0.21	3.80	0.09	0.68	0.06	0.46	49.60	12.34	85.44
13	LZ13	19.94	1.05	11.14	0.80	3.98	0.16	0.90	0.17	0.67	50.61	10.58	82.37
14	LZ14	20.18	1.46	10.66	0.92	3.40	0.16	0.83	0.26	0.69	52.41	9.04	80.08
Vigan River system													
15	LZ16	20.43	0.94	9.06	0.63	2.52	0.09	0.31	0.23	0.67	53.39	11.73	87.56
16	LZ17	19.59	1.55	8.71	0.77	2.92	0.09	0.51	0.23	0.70	54.43	10.49	81.28
17	LZ18	19.26	1.04	8.84	0.80	2.81	0.18	0.43	0.28	0.63	55.27	10.46	84.73
18	LZ19	20.07	1.05	9.02	0.72	3.32	0.09	0.54	0.34	0.63	51.16	13.06	84.85
19	LZ20	16.87	2.30	9.13	1.02	4.04	0.13	0.62	0.19	0.67	55.06	9.97	72.77
20	LZ21	18.39	1.80	9.02	1.07	3.38	0.11	0.41	0.17	0.60	55.15	9.90	78.25
21	LZ22	22.64	1.22	9.57	0.53	2.41	0.13	0.63	0.20	0.82	48.28	13.57	85.51
22	LZ24	20.39	1.36	11.24	0.38	3.03	0.15	0.66	0.23	0.81	50.44	11.30	83.64
23	LZ25	19.48	1.98	10.10	0.55	2.87	0.12	0.58	0.22	0.87	49.65	13.59	79.07
Cagayan River system													
24	LZ30	20.97	1.40	10.34	0.77	3.64	0.17	0.82	0.30	0.83	48.25	12.50	81.58
25	LZ31	20.80	1.30	10.03	0.76	2.30	0.15	0.32	0.19	0.83	51.68	11.64	84.80
26	LZ32	18.57	2.53	10.54	0.76	2.98	0.17	0.37	0.16	0.86	51.26	11.80	75.46
27	LZ33-1	21.59	1.24	11.26	0.79	2.40	0.11	0.52	0.24	0.88	50.19	10.77	84.46

(*continued on next page*)

Table 4 (*continued*)

No.	Sample	Al_2O_3	CaO	Fe_2O_3	K_2O	MgO	MnO	Na_2O	P_2O_5	TiO_2	SiO_2	LOI	CIA
28	LZ34	18.19	1.66	10.19	1.49	3.38	0.13	0.68	0.19	0.82	53.57	9.71	75.95
29	LZ35	18.87	1.78	9.75	1.34	2.95	0.14	0.39	0.23	0.80	52.72	11.02	77.91
30	LZ36	19.16	1.40	9.43	1.23	2.38	0.17	0.26	0.20	0.77	52.99	11.99	81.60
31	LZ37	21.66	0.57	9.67	0.75	1.52	0.14	0.25	0.22	0.95	51.82	12.45	90.47
32	LZ38	20.43	1.11	9.54	0.71	1.56	0.48	0.24	0.22	0.90	51.79	13.00	86.47
33	LZ39	20.03	1.09	11.26	1.30	1.32	0.45	0.36	0.30	0.91	51.81	11.18	83.41
34	LZ40	19.60	2.12	9.75	0.97	3.40	0.17	0.79	0.22	0.83	51.88	10.27	75.91
35	LZ41	21.94	1.10	10.74	0.54	2.16	0.17	0.46	0.21	0.78	49.53	12.37	86.76

LOI = loss of ignition. The samples were decarbonated before the chemical analysis.
SiO_2% = 100% – (All other major elements% + LOI), see text of analytical methods for more information.

sediments are more depleted in all major elements except P than bulk sediments. As indicated in major element compositions (Fig. 5, Table 4), clay-fraction sediments contain lower SiO_2, CaO, K_2O, Na_2O, MnO and MgO contents than bulk sediments. This situation results from the leaching of mobile elements K, Na and Ca and less mobile elements Si, Mn, and Mg during the formation of clay minerals under increasing degrees of the chemical weathering. The mobility of Si is critical for the understanding of chemical weathering processes. The SiO_2 content is depleted in both bulk and clay-fraction sediments, suggesting that moderate to strong chemical weathering processes occur in all Luzon rivers. The immobile Fe and Ti and less mobile Mn and Mg are markedly enriched in all river sediments, suggesting their common source from ferromagnesian minerals. The results fit very well the major lithology of andesitic–basaltic volcanic rocks and the predominant occurrence of smectite. The highly mobile elements Ca, Na and K from both bulk and clay-fraction sediments show lowest values related to their chemical weathering. Ca and Na are tightly held in feldspar (e.g., anorthite, albite) and K in orthoclase and micaceous minerals. With the chemical weathering mainly of andesitic–basaltic volcanic rocks, anorthite and albite contents can decrease dramatically from bulk to clay-fraction sediments, while orthoclase

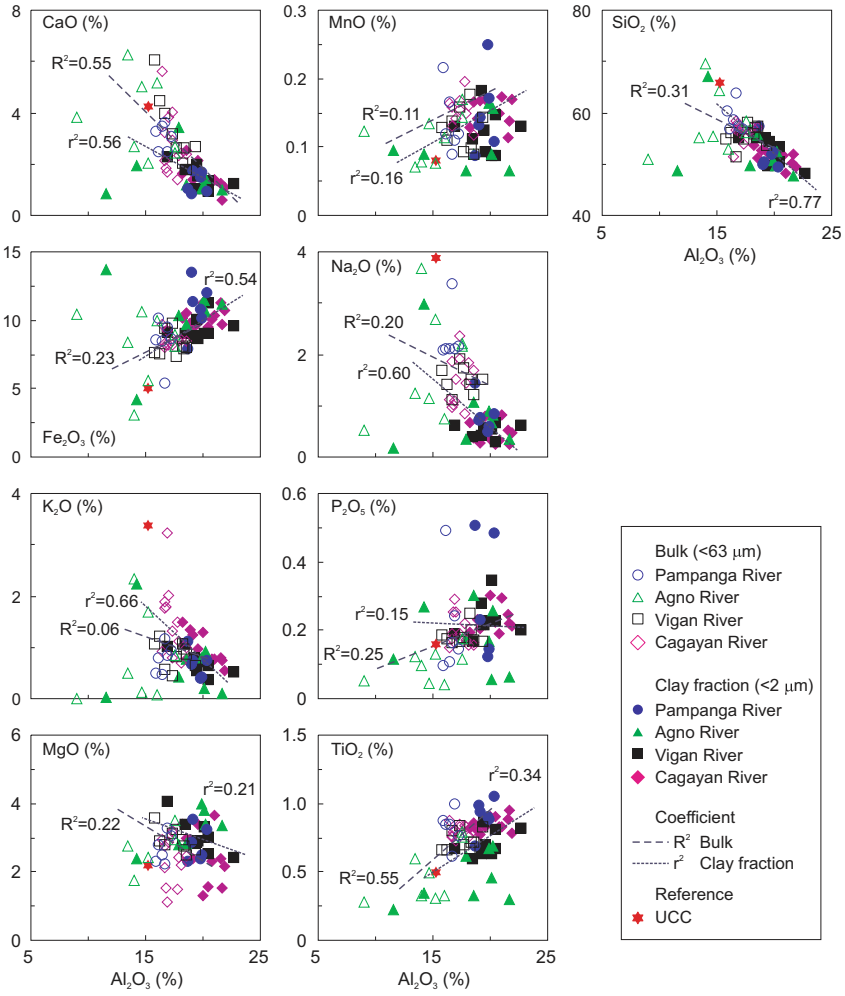

Fig. 5. Variation diagrams of major elements of bulk and clay-fraction sediments in Luzon rivers. Data of upper continental crust (UCC) from Taylor and McLennan (1985) were also plotted as a reference. Dashed lines indicate correlations with a coefficient R^2 for bulk sediments and r^2 for clay-fraction sediments, respectively. See Table 4 for major element compositions.

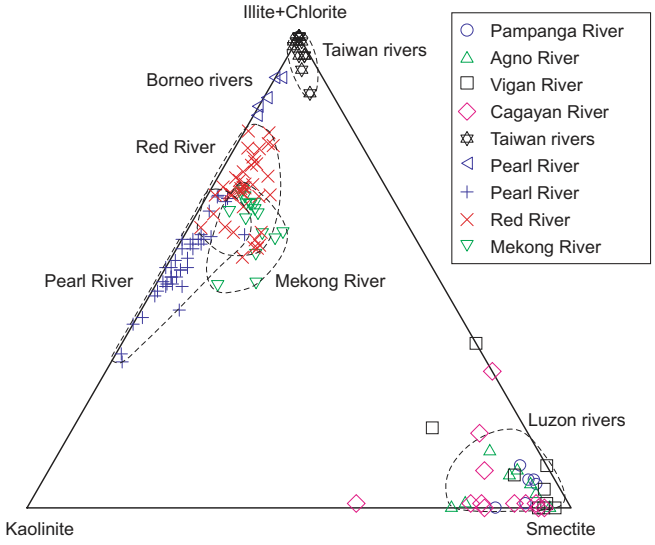

Fig. 6. Ternary diagram of clay mineral assemblages of surface sediments in Luzon rivers and their comparison with those in the Pearl, Red, Mekong, Taiwan and Borneo rivers. Clay mineral data for Pearl, Red and Mekong rivers from Liu et al. (2007a), data for Taiwan rivers from Liu et al. (2008), data for Borneo rivers from Liu et al. (2007b). All the referred literature data were generated using exactly the same analytical and calculation methods as in this study by the same research group so giving consistency of data comparison.

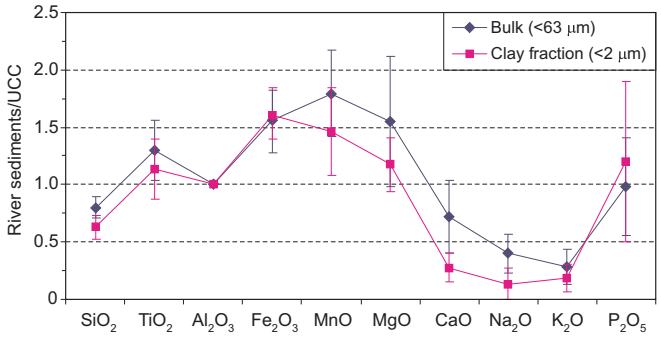

Fig. 7. Elemental ratios of bulk and clay-fraction sediments in Luzon rivers, calculated from average major-element concentrations normalized to UCC (Taylor and McLennan, 1985) with respect to Al_2O_3. The error bar for each element refers to the standard deviation of all samples.

and micaceous minerals are less abundant in both bulk and clay-fraction particles.

The degree of chemical weathering can be estimated by the chemical index of alteration (CIA) (Nesbitt and Young, 1982):

$$CIA = [Al_2O_3/(Al_2O_3 + CaO^* + Na_2O + K_2O)] \times 100,$$

where CaO^* represents CaO associated with the silicate fraction of the sample. For primary minerals (non altered minerals), all feldspars have CIA value of 50 and the mafic minerals biotite, hornblende and pyroxenes have CIA values between of 50–55, 10–30, and 0–10, respectively. Feldspar and mica weathering to smectite and kaolinite result in a net loss of K and Na in weathering profiles, whereas Al is resistant and is enriched in weathering products (Nesbitt and Young, 1982). This induces an increase of CIA values by about 100 for kaolinite and 70–85 for smectite. The CIA value is thought to quantify the state of chemical weathering of the rocks by referring to the loss of mobile elements such as Na, Ca and K. The results show that CIA values are 50–75 for bulk sediments and 75–90 for clay-fraction sediments (Fig. 8). An increase of about 15 CIA points is observed for clay-fraction sediments to bulk sediments. Among the different river systems (Fig. 8), relatively lower values of CIA in both bulk and clay-fraction sediments and lower smectite crystallinity are found in the Agno River system, confirming the provenance from ultrabasic intrusive rocks. No significant difference of CIA and smectite crystallinity is observed in the other three river systems. A moderate linear correlation of CIA with smectite crystallinity exists for clay-fraction sediments. A higher CIA value corresponds to a lower smectite crystallinity (a higher value), indicating stronger hydrolysis and vice versa. The results demonstrate that the degree of chemical weathering is moderate to intensive for clay-fraction sediments and low to moderate for bulk sediments. The bulk chemical weathering intensity in Luzon is much lower than in South China, where the major elemental and clay mineralogical data show intensive chemical weathering (Liu et al., 2007a), and even lower than in Taiwan where the chemical weathering is moderate (Selvaraj and Chen, 2006). From the linear correlation of CIA with smectite crystallinity (Fig. 8), values of smectite crystallinity above ~0.8°Δ2θ indicate intensive weathering and below ~0.8°Δ2θ moderate weathering in the case of clay-fraction sediments in Luzon rivers.

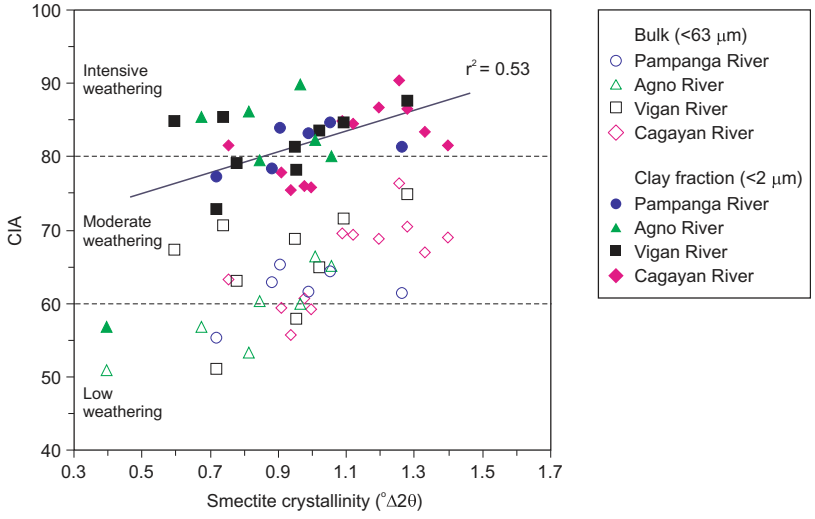

Fig. 8. Chemical index of alteration (CIA) of bulk and clay-fraction sediments and its correlation with smectite crystallinity of clay-fraction sediments in Luzon rivers. Dashed line indicates correlation with a coefficient (r^2).

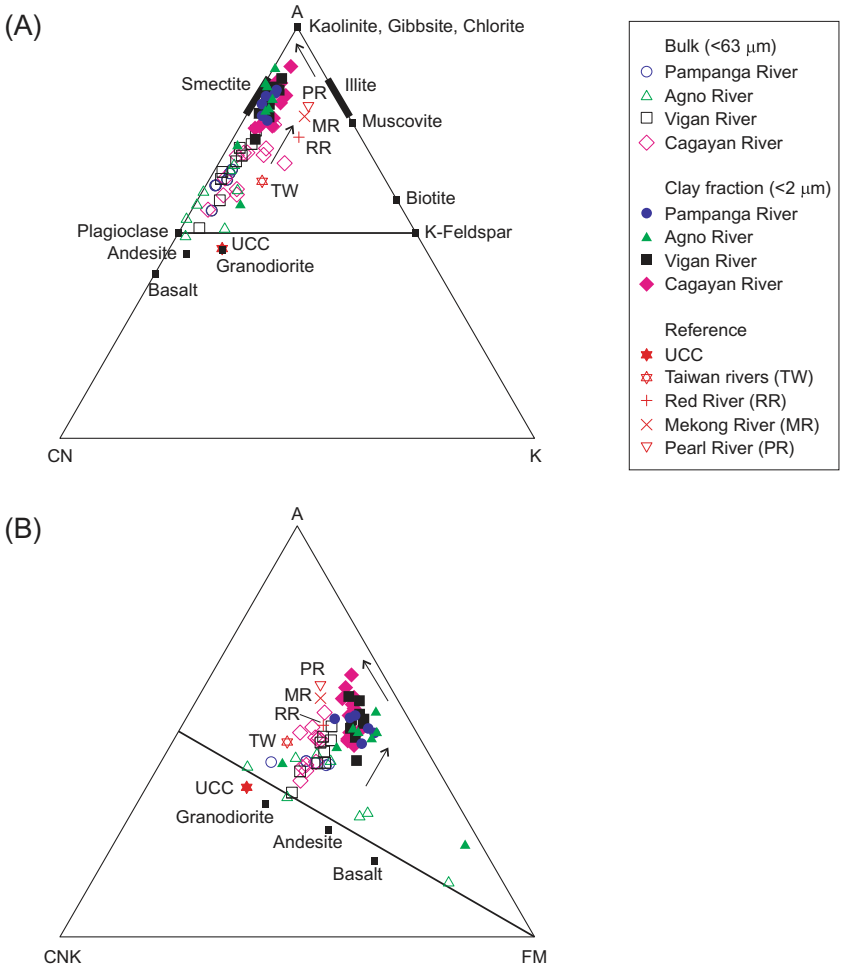

Fig. 9. Weathering trends from: (A) A–CN–K and (B) A–CNK–FM ternary diagrams of bulk and clay-fraction sediments in Luzon rivers. A = Al_2O_3; C = CaO; N = Na_2O; K = K_2O; F = total Fe; M = MgO. Average data for Pearl, Red and Mekong rivers (Liu et al., 2007a) and Taiwan rivers (Liu et al., 2008) are plotted for comparison; UCC (Taylor and McLennan, 1985) was also plotted as a reference. Arrows indicate weathering trends exhibited by these river sediments, showing that clay-fraction sediments have experienced stronger chemical weathering than bulk sediments.

Weathering trends in both bulk and clay-fraction sediments from all major to moderate rivers in Luzon can be clearly observed on Al_2O_3–(CaO + Na_2O)–K_2O (A–CN–K) and Al_2O_3–(CaO + Na_2O + K_2O)–(FeO + MgO) (A–CNK–FM) ternary diagrams (Nesbitt and Young, 1984, 1989) (Fig. 9). All samples plot linearly parallel to the A–CN or A–CNK line, with clay-fraction samples closer to the Al_2O_3 apex, indicating preferential leaching of CaO and Na_2O and enrichment of Al_2O_3, while K_2O contents (less abundant) are constant. Loss of CaO and Na_2O in clay-fraction sediments is very distinguishable, agreeing with the elemental mobility results (Fig. 7). The distribution of data plots close to the A–CN line (Fig. 9A) suggests a majority of andesitic–basaltic volcanic rock sources. The plots of clay-fraction sediments are very close to the smectite reference-segment in the A–CN–K diagram (Fig. 9A), reflecting the predominance of smectite in clay mineral assemblages of all river sediments (Fig. 2B). Further in the A–CNK–FM diagram (Fig. 9B), clay-fraction sediments tend to approach and then run parallel to the A–FM line, indicating leaching variability in FeO and MgO. Among the different river systems (Fig. 9), a slightly closer position to source rocks for bulk sediments is observed in the Agno River system, especially for some samples closer to the FM apex, confirming the source from ultrabasic intrusive rocks. No other significant difference of weathering trends is observed in the other three river systems. The comparison of weathering trends of Luzon river sediments with weathering states of UCC-like source rocks of the Pearl, Red, Mekong, and Taiwan rivers (Liu et al., 2007a, 2008) further determines their provenance from andesitic–basaltic volcanic rocks with associated ultrabasic intrusive rocks (Fig. 9).

6. Conclusions

Clay mineral assemblages and major element compositions have been studied for the first time on surface sediments in all 21 major to moderate rivers of Luzon to evaluate the present chemical weathering process. It is concluded that:

1. The clay mineral assemblage consists dominantly of smectite (average 86%) with minor amounts of kaolinite (9%) and chlorite (5%) and very scarce illite (1%). Low concentrations of halloysite, saponite, anorthite, talc, clinochrysotile, and clinoptilolite in clay fractions also occur in some locations. Their respective distribution does not show strong island-wide differences but with a slight increase in smectite (+3%) in the Pampanga River system in southern Luzon and a slight decrease in smectite (−3%) in the Cagayan River system in northern Luzon.
2. The mostly andesitic–basaltic volcanic and sedimentary rocks along with the tectonically active geological setting (active strike-slip faults, active volcanism and high seismic activity) and sub-tropical East Asian monsoon climate are responsible for the predominance of smectite associated with minor kaolinite in the clay mineral assemblage during rapid chemical weathering of rock surfaces in Luzon.

3. The elemental mobility and weathering trends of both bulk and clay-fraction sediments confirm the andesitic–basaltic volcanics with associated ultrabasic intrusives as source rocks in the hinterland. The formation of clay minerals with the predominance of smectite by chemical weathering is accompanied by leaching of Ca and Na first and of Fe and Mn thereafter. The CIA results combined with smectite crystallinity demonstrate a low-moderate chemical weathering degree of bulk sediments and a moderate-intensive degree of clay-fraction sediments in all investigated Luzon rivers.

Acknowledgments

We thank Peter B. Zamora for assistance during the fieldwork and Peijun Qiao and Lei Shao for technical help in the laboratories. Dr. Nathalie Fagel, Dr. Mark Hodson and one anonymous reviewer are thanked for their constructive reviews on the earlier version of this paper. This study was supported by the National Basic Research Program of China (2007CB815906), the National Natural Science Foundation of China (40925008, 40776027, 40876024, and 40621063), the Shanghai Rising-Star Program (07QH14014), the Shanghai Shuguang Program (07SG23), and the Doctoral Program of Higher Education of the Ministry of Education of China (20060247032).

References

Bellon, H., Yumul Jr., G.P., 2001. Miocene to Quaternary adakites and related rocks in western Philippine arc sequences. C.R. Acad. Sci. Paris Sci. Terre Planèt. 333, 343–350.

Biscaye, P.E., 1965. Mineralogy and sedimentation of recent deep-sea clay in the Atlantic Ocean and adjacent seas and oceans. Geol. Soc. Am. Bull. 76, 803–832.

Bluth, G.J.S., Kump, L.R., 1994. Lithologic and climatic controls of river chemistry. Geochim. Cosmochim. Acta 58, 2341–2359.

Boulay, S., Colin, C., Trentesaux, A., Frank, N., Liu, Z., 2005. Sediment sources and East Asian monsoon intensity over the last 450 kyr—mineralogical and geochemical investigations on South China Sea sediment. Palaeogeogr. Palaeoclimatol. Palaeoecol. 228, 250–277.

Chamley, H., 1989. Clay Sedimentology. Springer, New York.

Commission for the Geological Map of the World, 1975. Geological World Atlas, scale 1:1,00,00,000. UN Educ. Sci. Cult. Org., Paris.

Dessert, C., Dupré, B., François, L.M., Schott, J., Gaillardet, J., Chakrapani, G.J., Bajpai, S., 2001. Erosion of Deccan Traps determined by river geochemistry: impact on the global climate and the $^{87}Sr/^{86}Sr$ ratio of seawater. Earth Planet. Sci. Lett. 188, 459–474.

Eiriksdottir, E.S., Louvat, P., Gislason, S.R., Óskarsson, N., Hardardóttir, J., 2008. Temporal variation of chemical and mechanical weathering in NE Iceland: evaluation of a steady-state model of erosion. Earth Planet. Sci. Lett. 272, 78–88.

Galy, A., France-Lanord, C., 1999. Weathering processes in the Ganges–Brahmaputra basin and the riverine alkalinity budget. Chem. Geol. 159, 31–60.

Harrison, P.J., Yin, K., Lee, J.H.W., Gan, J., Liu, H., 2008. Physical–biological coupling in the Pearl River Estuary. Continent. Shelf Res. 28, 1405–1415.

Holtzapffel, T., 1985. Les minéraux argileux: préparation, analyse diffractométrique et determination. Soc. Géol. Nord Publ. 12.

Kleber, M., Schwendenmann, L., Veldkamp, E., Rößner, Jahn R., 2007. Halloysite versus gibbsite: silicon cycling as a pedogenetic process in two lowland neotropical rain forest soils of La Selva, Costa Rica. Geoderma 138, 1–11.

Liu, Z., Colin, C., Trentesaux, A., Blamart, D., Bassinot, F., Siani, G., Sicre, M.-S., 2004. Erosional history of the eastern Tibetan Plateau over the past 190 kyr: clay mineralogical and geochemical investigations from the southwestern South China Sea. Mar. Geol. 209, 1–18.

Liu, Z., Colin, C., Huang, W., Le, K.P., Tong, S., Chen, Z., Trentesaux, A., 2007a. Climatic and tectonic controls on weathering in South China and the Indochina Peninsula: clay mineralogical and geochemical investigations from the Pearl, Red, and Mekong drainage basins. Geochem. Geophys. Geosyst. 8, Q05005. doi:10.1029/2006GC001490.

Liu, Z., Zhao, Y., Li, J., Colin, C., 2007b. Late Quaternary clay minerals off Middle Vietnam in the western South China Sea: Implications for source analysis and East Asian monsoon evolution. Sci. China Ser. D Earth Sci. 50, 1674–1684.

Liu, Z., Tuo, S., Colin, C., Liu, J.T., Huang, C.-Y., Selvaraj, K., Chen, C.-T.A., Zhao, Y., Siringan, F.P., Boulay, S., Chen, C., 2008. Detrital fine-grained sediment contribution from Taiwan to the northern South China Sea and its relation to regional ocean circulation. Mar. Geol. 255, 149–155.

Louvat, P., Allègre, C.J., 1998. Riverine erosion rates on Sao Miguel volcanic island, Azores archipelago. Chem. Geol. 148, 177–200.

McLennan, S.M., 1993. Weathering and global denudation. J. Geol. 101, 295–303.

Milliman, J.D., Meade, R.H., 1983. World-wide delivery of sediment to the oceans. J. Geol. 91, 1–21.

Milliman, J.D., Syvitski, J.M.P., 1992. Geomorphic/tectonic control of sediment discharge to the ocean: the importance of small mountainous rivers. J. Geol. 100, 525–544.

Nesbitt, H.W., Young, G.M., 1982. Early Proterozoic climates and plate motions inferred from major element chemistry of lutites. Nature 299, 715–717.

Nesbitt, H.W., Young, G.M., 1984. Prediction of some weathering trends of plutonic and volcanic rocks based on thermodynamic and kinetic considerations. Geochim. Cosmochim. Acta 48, 1523–1534.

Nesbitt, H.W., Young, G.M., 1989. Formation and diagenesis of weathering profiles. J. Geol. 97, 129–147.

Nesbitt, H.W., Mackovics, G., Price, R.C., 1980. Chemical processes affecting alkalis and alkaline Earth during continental weathering. Geochim. Cosmochim. Acta 44, 1659–1666.

Petschick, R., 2000. MacDiff 4.2.2 [Online]. <http://servermac.geologie.uni-frankfurt.de/Rainer.html> (cited 01.12.01).

Rimando, R.E., Knuepfer, P.L.K., 2006. Neotectonics of the Marilina Valley fault system (MVFS) and tectonic framework of structures in northern and central Luzon, Philippines. Tectonophysics 415, 17–38.

Selvaraj, K., Chen, C.-T.A., 2006. Moderate chemical weathering of subtropical Taiwan: constraints from solid-phase geochemistry of sediments and sedimentary rocks. J. Geol. 114, 101–116.

Singh, M., Sharma, M., Tobschall, H.L., 2005. Weathering of the Ganga alluvial plain, northern India: implications from fluvial geochemistry of the Gomati River. Appl. Geochem. 20, 1–21.

Summerfield, M.A., Hulton, N.J., 1994. Natural controls of fluvial denudation rates in major world drainage basins. J. Geophys. Res. 99, 13871–13883.

Taylor, S.R., McLennan, S.M., 1985. The Continental Crust: Its Composition And Evolution. Blackwell, Malden, Mass.

Vital, H., Stattegger, K., 2000. Major and trace elements of stream sediments from the lowermost Amazon River. Chem. Geol. 168, 151–168.

Walker, J.C.G., Hays, P.B., Kasting, J.F., 1981. A negative feedback mechanism for the long-term stabilization of Earth's surface temperature. J. Geophys. Res. 86, 9776–9782.

Wan, S., Li, A., Clift, P.D., Stuut, J.-B.W., 2007. Development of the East Asian monsoon: mineralogical and sedimentologic records in the northern South China Sea since 20 Ma. Palaeogeogr. Palaeoclimatol. Palaeoecol. 254, 561–582.

Yang, S., Jung, H.-S., Li, C., 2004. Two unique weathering regimes in the Changjiang and Huanghe drainage basins geochemical evidence from river sediments. Sediment. Geol. 164, 19–34.